Received: 11 January 2019 | Revised: 1 April 2019 | Accepted: 2 April 2019

DOI: 10.1002/nau.24008

ORIGINAL BASIC SCIENCE ARTICLE

WILEY Neurourology Urodynamics ICS SUFU

Time-dependent functional, morphological, and molecular changes in diabetic bladder dysfunction in streptozotocin-induced diabetic mice

Xu-feng Yang[1] | Jing Wang[1] | Rui-Wang[1] | Yi-fei Xu[1] | Fang-jun Chen[1] | Li-yao Tang[1] | Wen-kang Ren[1] | Li-jun Fu[1] | Bo Tan[3] | Ping Huang[1,2] | Hong-ying Cao[1,2]

[1]Department of pharmacology of Chinese Medicine, School of Pharmaceutical Sciences, Guangzhou University of Chinese Medicine, Guangzhou, China

[2]Dongguan & Guangzhou University of Chinese Medicine Cooperative Academy of Mathematical Engineering for Chinese Medicine, Guangzhou University of Chinese Medicine, Dongguan, China

[3]School of Basic Medical Sciences, Guangzhou University of Chinese Medicine, Guangzhou, China

Correspondence
Prof. Ping Huang and Prof. Hong-Ying Cao, Department of Pharmacology of Chinese Medicine, School of Pharmaceutical Sciences, Guangzhou University of Chinese Medicine, Guangzhou, China.
Email: hping331@126.com (P.H.); 1171629708@qq.com (H.Y.)

Funding information
Dongguan Municipal Science and Technology Bureau, Grant/Award Number: 2019622101002; National Natural Science Foundation of China, Grant/Award Number: 81673676; Dongguan Science and Technology Bureau, Grant/Award Number: 2019622101002

Abstract

Aim: Diabetic bladder dysfunction (DBD) is one of the most common and bothersome complications of diabetes mellitus (DM). This study aimed to investigate the functional, structural, and molecular changes of the bladder at 0, 3, 6, 9, and 12 weeks after DM induction by streptozotocin (STZ) in male C57BL/6 mice.

Methods: Male C57BL/6J mice were injected with STZ (130 mg/kg). Then, diabetic general characteristics, cystometry test, histomorphometry, and contractile responses to α, β-methylene ATP, KCl, electrical-field stimulation, carbachol were performed at 0, 3, 6, 9, and 12 weeks after induction. Finally, protein and messenger RNA (mRNA) expressions of myosin Va and SLC17A9 were quantified.

Results: DM mice exhibited lower body weight, voiding efficiency and higher water intake, urine production, fasting blood glucose, oral glucose tolerance test, bladder wall thickness, maximum bladder capacity, residual volume, bladder compliance. In particular, nonvoiding contractions has increased more than five times at 6 weeks. And the amplitudes of spontaneous activity, contractile responses to all stimulus was about two times higher at 6 weeks but cut almost in half at 12 weeks. The protein and mRNA expressions of myosin Va and SLC17A9 were about two times higher at 6 weeks, but myosin Va was reverted nearly 40% while SLC17A9 is still higher at 12 weeks.

Conclusions: DBD transitioned from a compensated state to a decompensated state in STZ-induced DM mice at 9 to 12 weeks after DM induction. Our molecular data suggest that the transition may be closely related to the alterations of myosin Va and SLC17A9 expression levels in the bladder with time.

Abbreviations: BC, bladder compliance; BG, blood glucose; BWT, bladder wall thickness; DBD, diabetic bladder dysfunction; DM, diabetes mellitus; DSM, detrusor smooth muscle; EFS, electrical-field stimulation; FBG, fasting blood glucose; MBC, maximum bladder capacity; MVP, maximum voiding pressure; NVCs, nonvoiding contractions; RV, residual volume; SD, standard deviation; STZ, streptozotocin; VE, voiding efficiency.

Xu-feng Yang and Jing Wang contributed equally to the study.

KEYWORDS

compensated state, decompensated state, diabetic bladder dysfunction (DBD), myosin Va, SLC17A9, temporal changes

1 | INTRODUCTION

Diabetes mellitus (DM) is a far-reaching endocrine metabolic disease affecting approximately 425 million individuals in 2017 according to the International Diabetes Federation. DM is characterized by chronic hyperglycemia accompanied by numerous deleterious complications, including a series of lower urinary tract diseases.[1] Diabetic bladder dysfunction (DBD) is a major DM complication in the lower urinary tract, affecting more than half of the patients with DM[2] and causing a range of storage and voiding problems clinically. DBD was firstly defined by Frimodt-Moller in 1976[3] and has been widely considered as some bladder dysfunction.[4,5] The classic DBD symptoms are decreased bladder sensation, augmented bladder capacity, and poor micturition efficiency.[6] However, an increasing number of studies reported the evidence of overactive bladder in patients with DM and DM animals.[7,8] Recently, the temporal theory of DBD was proposed to explain the contradictory symptoms of patients and was demonstrated in some animal experiments,[9-11] and viewed that DBD comprises two states: a compensated state, which occurs soon after the onset of diabetes, characterized by overactive detrusor, increased contractility; and followed by a decompensated state, which develops at the later stages of diabetes, featured by decreased peak and poor emptying.[9,12]

Clinically, controlling blood glucose (BG) level is the basis of treatment, but it cannot completely eliminate DBD.[13] The treatment varies with DBD progression; muscarinic receptor antagonists, such as tolterodine, are used to ameliorate the symptoms of an overactive bladder, whereas surgical intervention is the most effective method for patients with chronic urine retention.[14] However, all these abovementioned treatments have numerous side effects. Despite the multitude of animal experiments and clinical studies that have explored the pathophysiology of DBD from different perspectives, such as urethra, autonomic nerves, detrusor muscle, its molecular mechanisms are still unclear. Therefore, the underlying molecular alterations, which can potentially be used for targeted therapies, need to be fully elucidated.

The bladder contraction is mediated by both neurogenically mediated cholinergic and nonadrenergic–noncholinergic (NANC) pathways, whereas ATP, the primary NANC excitatory transmitter, induces the purinergic contraction.[14] At present, considerably numerous articles have reported that a purinergic-induced bladder contraction is dramatically changed in patients and animals with DM.[15] However, whether the alteration of purinergic-induced contraction in DM conditions is related to the change of ATP release remains poorly studied. ATP as the purinergic transmitter is principally released by an exocytotic process; this process requires a previous reserve in vesicles and is mediated by vesicular nucleotide transporter (VNUT),[16] confirmed to be SLC17A9.[17] Furthermore, the exocytotic process requires transfer from the neurotransmitter-filled vesicles to the varicosity membrane and is mainly mediated by myosin Va.[18] Hence, this study aimed to explore the functional and morphological alterations in different development processes of DBD and the contributions of myosin Va and SLC17A9 changes to the bladder's contractility alterations in STZ-induced DM mice.

2 | MATERIALS AND METHODS

2.1 | Animal model

One hundred and sixty male C57BL/6J mice (6 weeks of age, 18–22 g) were randomly assigned to two groups by using random number table, namely, DM (n = 85) and control (n = 75) groups. And all mice were housed at room temperature 25 ± 2℃) with 12 hours light and dark cycles. The DM mice were injected with STZ (130 mg/kg). Fasting blood glucose (FBG) test was measured 48 hours after injection of STZ and the mice with FBG ≥ 11.1 mmol/L were considered as the DM model mice. Then, the DM mice were randomly divided into five groups, namely, 0-, 3-, 6-, 9-, and 12-week model groups (n = 15). The control mice were also divided into the corresponding groups (n = 15).

2.2 | Measurements of weight, water intake, urine production, and frequency

At 0, 3, 6, 9, and 12 weeks, the mice were placed individually in metabolic cages. Then, water intake was measured within 24 hours of water consumption. The frequency of urination was obtained by measuring the

5 hours voided stain on paper test papers, and urine production was measured by evaluating the area of voided stain under ultraviolet light.

2.3 | FBG test and oral glucose tolerance test

At 0, 3, 6, 9, and 12 weeks, FBG and oral glucose tolerance test were measured. The tests were measured after fasting for 12 hours. After glucose (2 mg/g body weight) administration via gavage, BG concentrations were measured at 0, 15, 30, 60, 90, and 120 minutes. Then, the BG AUC_{0-2h} was calculated.

2.4 | Cystometry test in vivo

The cystometry data was measured by using urodynamics meter. After anesthetizing the mice by intraperitoneally injecting of 25% urethane (1.25–1.50 g/kg), a 25-gauge needle was inserted into the bladder dome. The needle was connected to a three-way adapter, which was linked with a microinjection pump at one end and a urodynamics meter at the other. The test was executed by pumping a 0.9% room-temperature saline solution into the bladder at 3 ml/h. The following cystometry parameters were assessed at 0, 3, 6, 9, and 12 weeks: maximum bladder capacity (MBC; the volume of saline pumped before the urination), maximum voiding pressure (MVP), the frequency of nonvoiding contractions (NVCs; higher than 5 cm H_2O spontaneous bladder contraction that did not result in urination before the urination), residual volume (RV; the volume remaining in the bladder after voiding, measured manually by using a 1 ml syringe to obtain the urine remaining in the bladder after voiding), voiding efficiency (VE; calculated as [(MBC − RV)/MBC] × 100%), and bladder compliance (BC; calculated as [(MBC/MVP) × 100%]). After the experiment, animals were euthanized by cervical dislocation. The data for the individual mouse represents the mean of three times voiding.[19]

2.5 | Histology

The mice were killed, after which the bladder was harvested and weighed. The bladders were soaked in 4% paraformaldehyde solution and then embedded into paraffin. Moreover, the bladders were transected along the transverse sections (6 μm) and stained with hematoxylin and eosin (H&E) and Masson's trichrome (100×). Bladder wall thickness (BWT) was determined by H&E images while Smooth muscle-to-collagen ratio calculated from the Masson's trichrome images, all images were processed and analyzed with special software (Image Pro 6.0). In the end, we looked at the histology slides that had been blinded with regard to the group allocation.

2.6 | Assessment of detrusor smooth muscle strips contractility in vitro

The full-thickness (the detrusor was fixed and quickly cut to retain the mucosa) longitudinal detrusor smooth muscle (DSM) strips (5–7 mm × 5 mm) were mounted in a 5 ml organ bath filled with Krebs-Henseleit solution (NaCl, 118 mM; KCl, 4.75 mM; $MgSO_4$, 1.18 mM; $NaHCO_3$, 24.8 mM; KH_2PO_3, 1.18 mM; $CaCl_2$, 2.5 mM; and $C_6H_{12}O_6{\cdot}H_2O$, 10 mM; pH, 7.4; 37°C) and bubbled with a gas mixture of 95% oxygen and 5% carbon dioxide. The resting tension was loaded at 0.5 g and the strips were equilibrated for 60 minutes. Then, amplitude and frequency of spontaneous activity were determined. In addition, the contractile response to α, β-methylene ATP (100 μM), KCl (120 mM), electrical-field stimulation (EFS, 1, 2, 4, 8, 16, 32, and 64 Hz; 40 V; and 0.5 ms pulse duration for 10 seconds), and carbachol (10^{-8} to 10^{-5} M) were measured. The carbachol curves were cumulative, and the base value used in carbachol analysis was the baseline immediately before the beginning of the curve. And pEC50 values were calculated according to the formula: $pEC50 = -\log_{10}^{(EC50)}$. In the end, the weight and length of each DSM strips were recorded, and the formula: [(peak value − base value)(g) × Length(mm) × 1.06 (mg/mm^3) × 0.0098(N/g)]/weight (g) was used to normalize the amplitude of contractility.

2.7 | Western blot analysis

The total protein of bladder tissues was extracted using tissue grinders, and the concentration was determined using the BCA protein assay kit. Then, the different molecular weights proteins (20 μg) were separated and transferred to a PVDF membrane. Subsequently, the membranes were incubated with primary antibodies overnight at 4°C. After bieng incubated with a secondary antibody, the target proteins were visualized by a chemiluminescence system. The immunoblot protein expression levels, namely, myosin Va and SLC17A9, were normalized by β-actin and quantified by ImageJ 1.8.0. The antibodies used are listed in Table 1.

2.8 | Real-time reverse transcription polymerase chain reaction

The total ribonucleic acid (RNA) was extracted using the TRIzol reagent. The RNA quality was evaluated by

TABLE 1 List of antibodies used for Western blot analysis

Antigen	Manufacturer	Dilution
β-actin	Santa Cruz, Cat: sc-365986 mouse monoclonal	1:1000
myosinVa	Santa Cruz, Cat: sc-365986 mouse monoclonal	1:1000
SLC17A9	MBL, Cat: BMP079 rabbit monoclonal	1:1000

ultraviolet absorption. Then, cDNA was obtained using the FastKing One-step RT-PCR (reverse transcription polymerase chain reaction) Kit, and real-time PCR analysis was performed using the Talent qPCR (quantitative polymerase chain reaction) PreMix (SYBR Green). The synthetic oligonucleotide primers were shown in Table 2. Myosin Va and SLC17A9 expression levels were individually calculated and normalized by $2^{-\Delta\Delta Ct}$ method according to the β-actin expression.

2.9 | Statistical analysis

Data were expressed as mean ± standard deviation in this study. The program SPSS 19.0 and GraphPad Prism 5 were used for statistical analysis. In this study, the unpaired student *t* test was performed, $P < 0.05$ was accepted as significant. All statistical intergroup comparisons had been preplanned and all statistical comparisons being performed are being reported irrespective of the outcome, that is, whether *P* was < 0.05 or not.

3 | RESULTS

3.1 | General characteristics of the DM model

The weights of DM mice gradually declined at 0 to 6 weeks but remained unchanged at 6 to 12 weeks, and were less than controls at 3 to 12 weeks. The water intake and urine production of the DM mice were more than doubled compared with controls at all time points ($P < 0.01$). Meanwhile, the frequency of urination in DM mice increased sharply from 0 to 6 weeks and then gradually decreased at the subsequent time, but the whole process was higher than that of the controls. In addition, the FBG ($P < 0.01$) and Bg $AUC_{0\text{-}2h}$ of DM mice consistently increased over time, and were more than doubled than that of the controls ($P < 0.01$) at all time points (Figure 1A-G).

TABLE 2 Primer sequences of β-actin, myosinVa, and SLC17A9

Gene	Primers (5′-3′)
β-actin - F	CTACCTCATGAAGATCCTGACC
β-actin - R	CACAGCTTCTCTTTGATGTCAC
myosinVa - F	AGCTCAACTCCTTCCACTC
myosinVa - R	ACACACCCCTTTATCCTTCC
SLC17A9 - F	GCTTCCTCAAGGCTATGATCTT
SLC17A9 - R	AGGTCCTGAATGTTGACTGAAA

3.2 | Cystometric studies

Cystometrogram tracings of DM and control mice were obtained at 0, 3, 6, 9 and 12 weeks (Figure 2A). Compared with controls, the MBC (Figure 2B), RV (Figure 2E), and BC (Figure 2G) of DM mice all steadily increased at 0 to 9 weeks, and the parameters dramatically rose at 9 to 12 weeks. Meanwhile, the MVP (Figure 2C) of DM mice did not markedly change with time and was close to the matched controls at 0 to 9 weeks, but it declined by a quarter compared with controls at 12 weeks ($P < 0.01$). In addition, the NVCs (Figure 2D) of DM mice were significantly higher at 3 to 9 weeks, especially at 6 weeks, reaching more than five-fold than those of controls ($P < 0.01$). Moreover, VE (Figure 3F) continuously decreased in DM mice at 0 to 12 weeks and was statistically lower than controls at 6 to 12 weeks.

3.3 | Morphometric analysis

The absolute (Figure 3B) and relative bladder weights (Figure 3C) in DM mice gradually increased. In addition, the morphometric analysis results showed that the bladder BWT (Figure 4D) of DM mice sharply increased at 0 to 6 weeks, but had not markedly increased at 6 to 12 weeks, and markedly increased compared with the controls at 3 to 12 weeks. The bladder smooth muscle-to-collagen ratio (Figure 5E) remained unchanged at all time points.

3.4 | In vitro contractility studies

The results showed a temporal alteration bladder function in DM mice. First, we found that the DMS strips of DM mice exhibited double higher amplitudes of spontaneous activity at 6 weeks (Figure 4A,B) than controls ($P < 0.01$), but cut almost in half at 12 weeks (Figure 4A,B) ($P < 0.05$). In addition, the frequency of bladder spontaneous activity in DM mice was stable relative to the matched controls (Figure 4C). The contractile responses to ATP (100 μM; Figure 4D) and KCL (120 mM; Figure 4E) were significantly greater in DM mice at 6 weeks but diminished at 12 weeks compared with controls. The contractile responses of DSM strips to EFS (1-64 Hz; Figure 4H), carbachol stimulation (10^{-8} to 10^{-5} M; Figure 4I) and

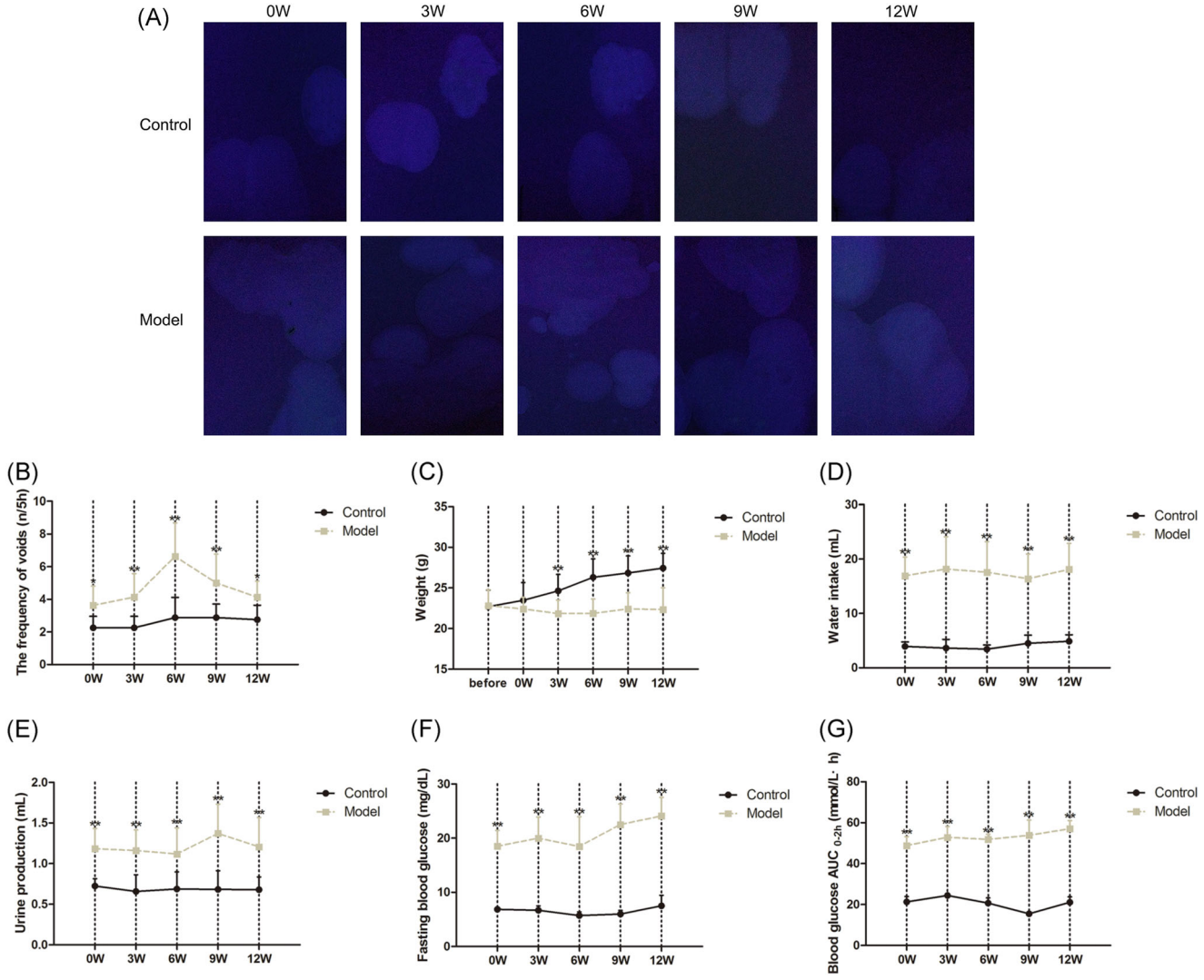

FIGURE 1 General characteristics of diabetes mellitus (DM) model and age-matched control mice from 0 to 12 weeks after the induction (n = 15). A, The image from 5 hours voided stain test, (B) 5 hours frequency of urination, (C) weight, (D) water intake, (E) 5 hours Urine production, (F) Fasting blood glucose (FBG), (G) Blood glucose (BG) AUC_{0-2h} (n = 15, according to the following formula: BG $AUC_{(0-2h)}$ = [(BG0 + BG15) × 0.5] ÷ 4 + [(BG15 + BG30) × 0.5] ÷ 4 + [(BG30 + BG60) × 0.5] ÷ 2 + [(BG60 + BG120) × 0.5]). Data represent the means ± SD (model vs control group, $^{**}P < 0.01$ or $^{*}P < 0.05$). SD, standard deviation

maximal responses (E_{max}) values (Figure 4G) to carbachol were double higher in DM mice at 6 weeks, but decreased 50% at 12 weeks relative to controls ($P < 0.01$ or $P < 0.05$) while potency (pEC50) to carbachol was steady (Figure 4F).

3.5 | Western blot analysis

The protein expression level of myosin Va (Figure 5B) was about two times higher in the bladder tissues of DM mice at 6 weeks ($P < 0.01$) but sharply decreased 40% at 12 weeks compared with the controls ($P < 0.05$). The protein expression level of SLC17A9 (Figure 5C) was markedly increased in the DM mice at 6, 9, and 12 weeks compared with controls.

3.6 | Real-time RT-PCR analysis

The messenger RNA (mRNA) expression level of myosin Va (Figure 5D) significantly increased about 50% times in the DM mice at 6 weeks ($P < 0.05$) but declined 40% at 12 weeks ($P < 0.05$) relative to controls. Meanwhile, the mRNA expression level of SLC17A9 (Figure 5E) increased about a third in the DM mice at 6 and 9 weeks ($P < 0.01$ or $P < 0.05$) compared with the controls.

4 | DISCUSSION

DBD, which is one of the most serious lower urinary tract complications of DM, is not life-threatening but substantially affects many aspects in the quality of a patient's

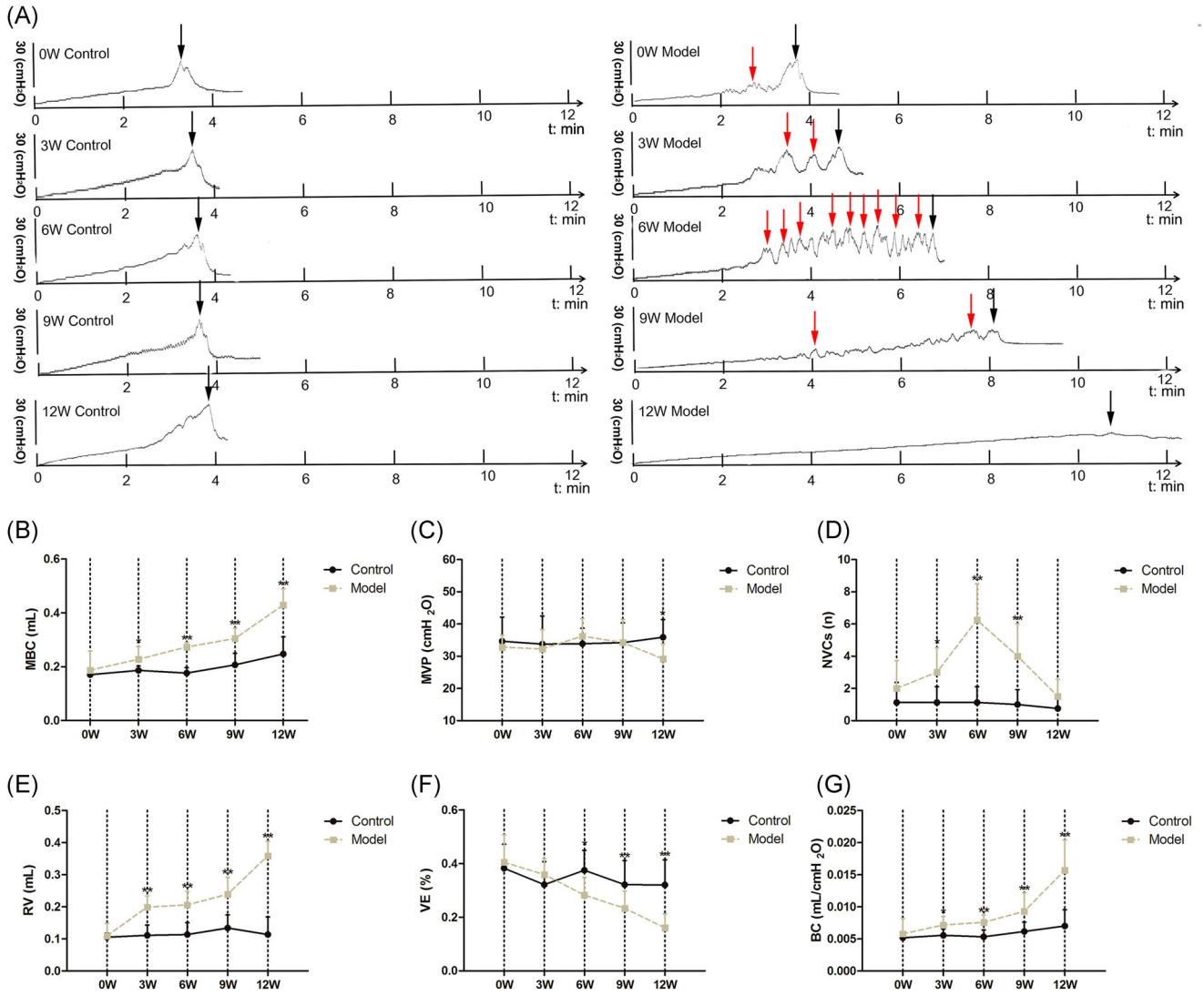

FIGURE 2 A, Representative cystometric recording from the age-matched control and DM mice from 0 to 12 weeks after the induction ($n = 8$). B, Maximum bladder capacity (MBC), (C) maximum voiding pressure (MVP), (D) the frequency of nonvoiding contractions (NVCs), (E) residual volume (RV), (F) voiding efficiency (VE, calculated as [(MBC − RV)/MBC] × 100%), (G) bladder compliance (BC; calculated as [(MBC/MVP) × 100%]). Data represent the means ± SD (model vs. control group, $^{*}P < 0.05$ or $^{**}P < 0.01$). Black arrows indicate the micturition peaks and red arrows represent the nonvoiding contractions (NVCs). DM, diabetes mellitus; SD, standard deviation

life and work.[12] Recently, the "temporal hypothesis," which holds that DBD mainly undergoes two phases of alterations via two mechanisms, has been gradually recognized and accepted by more people, with time-dependent functional and morphological manifestations of DBD found in patients with DBD and STZ-induced DM mice.[9] It pointed out a scientific way to explore the mechanism of DBD on which the underlying molecular pathways may be changing with time. However, the mechanisms of DBD translation remain elusive.

In our study, the model mice showed a series of characteristics of DM, such as abnormal carbohydrate metabolism and high BG levels, suggesting that the DM model was established successfully. Bladder disorders are commonly categorized as storage or voiding problems, which can be qualified and quantified by urodynamic parameters. Bladder overactivity or instability is characterized by sensory urgency and higher NVCs frequency, whereas voiding problems indicate decreased MVP and VE, and increased RV.[20] The cystometric test results clearly showed that the DM mice entered the compensated state at 6 weeks was characterized by sharply increased NVCs; subsequently, the decompensated state at 12 weeks was characterized by increased MBC, RV, and BC, and dramatically reduced MVP and VE, conforming to the previous studies.[9] In addition, BWT, absolute and relative bladder weights of the DM mice persistently increased with the time, which are consistent with the increase in bladder capacity and prevised studies,[21,22] thereby possibly reflecting a

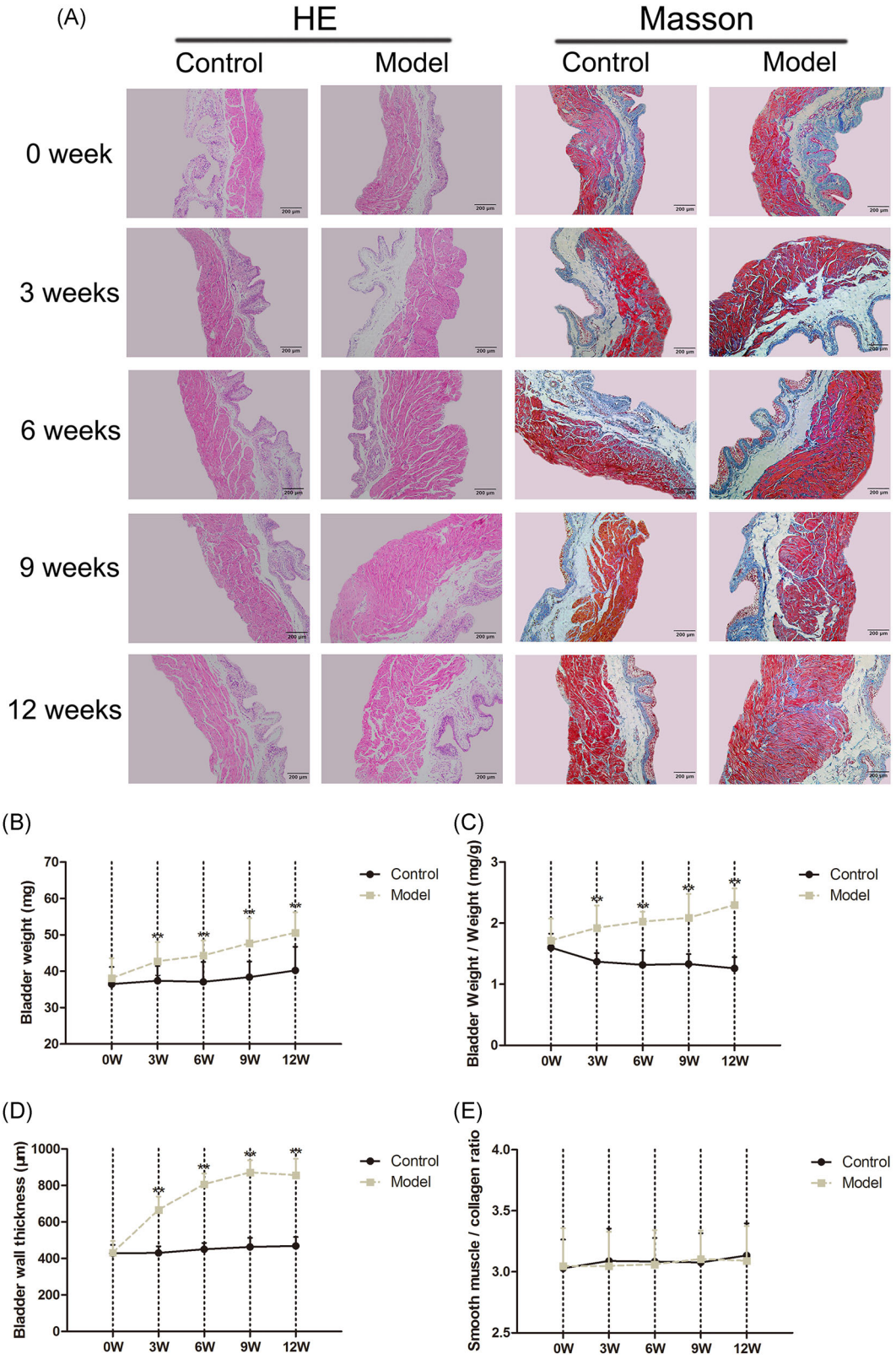

FIGURE 3 Absolute and relative bladder weights of the age-matched control and DM mice from 0 to 12 weeks after induction (n = 15). A, Bladder weight, (B) bladder-weight-to-body-weight ratio; H&E and Masson's trichrome staining digital images (100×) of the age-matched control and DM mice from 0 to 12 weeks after the induction (n = 7). C, Bladder wall thickness (BWT) determined by H&E images, (D) smooth muscle-to-collagen ratio calculated from the Masson's trichrome images. All images were processed and analyzed with special software (Image Pro 6.0) (model vs control group, $^{*}P < 0.05$ or $^{**}P < 0.01$). DM, diabetes mellitus; H&E, hematoxylin and eosin

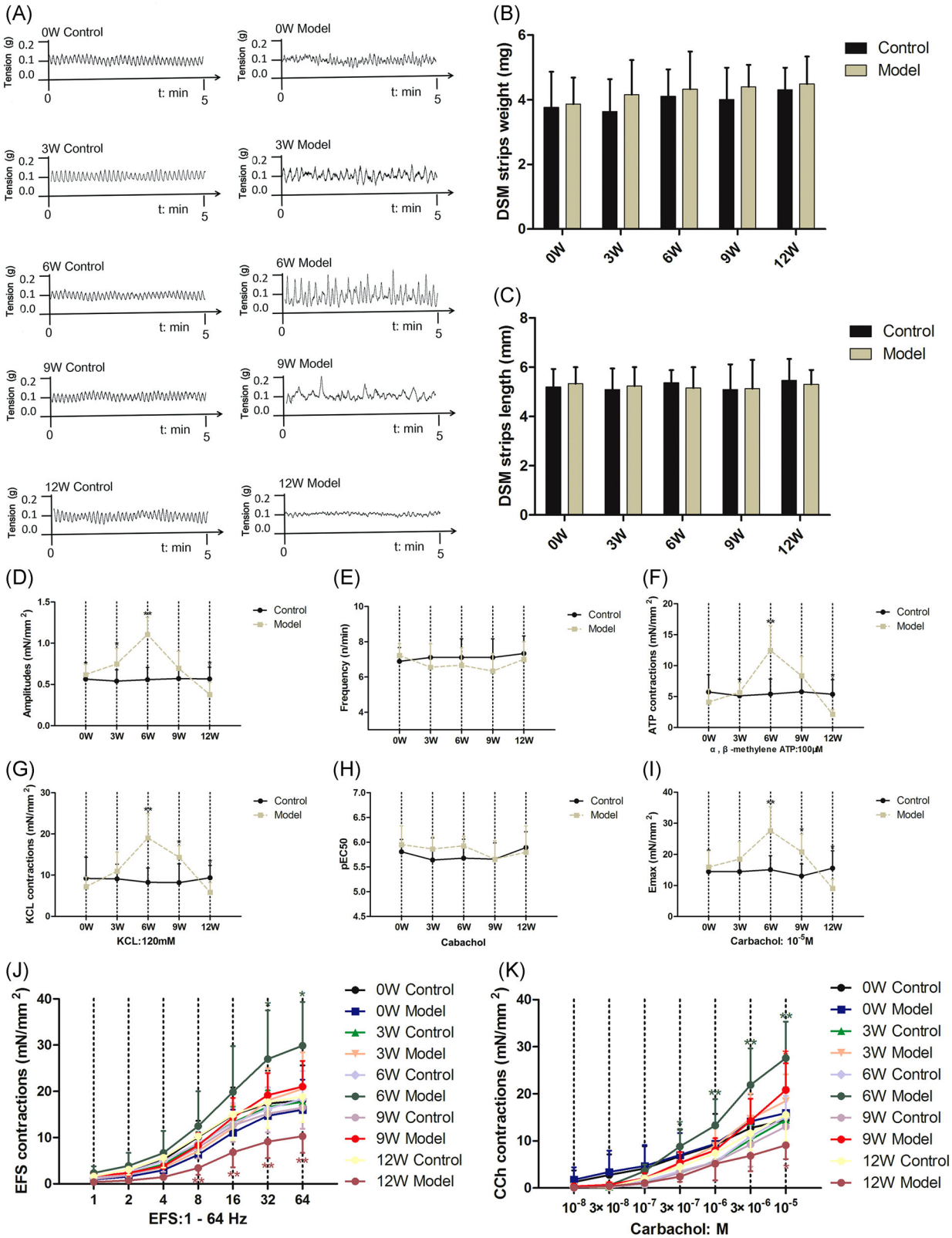

FIGURE 4 A, Amplitudes and frequency of spontaneous activity in detrusor smooth muscle (DSM) of the age-matched control and DM mice from 0 to 12 weeks after the induction (n = 14). Detrusor smooth muscle (DSM), (B) weight, and (C) length of all groups. D, Amplitudes of spontaneous activity, (E) frequency of spontaneous activity; DSM contraction in response to (F) α, β-methylene ATP (100 μM), (G) KCl (120 mM), (J) electrical-field stimulation (EFS, 1–64 Hz) and (K) carbachol (10^{-8} to 10^{-5} M) in the age-matched control and DM mice from 0 to 12 weeks after induction. H, Potency (pEC50) and (I) maximal responses (E_{max}) values obtained from concentration-response curves to carbachol. Data represent the means ± SD (model vs. control group, $^{*}P < 0.05$ or $^{**}P < 0.01$). DM, diabetes mellitus; SD, standard deviation

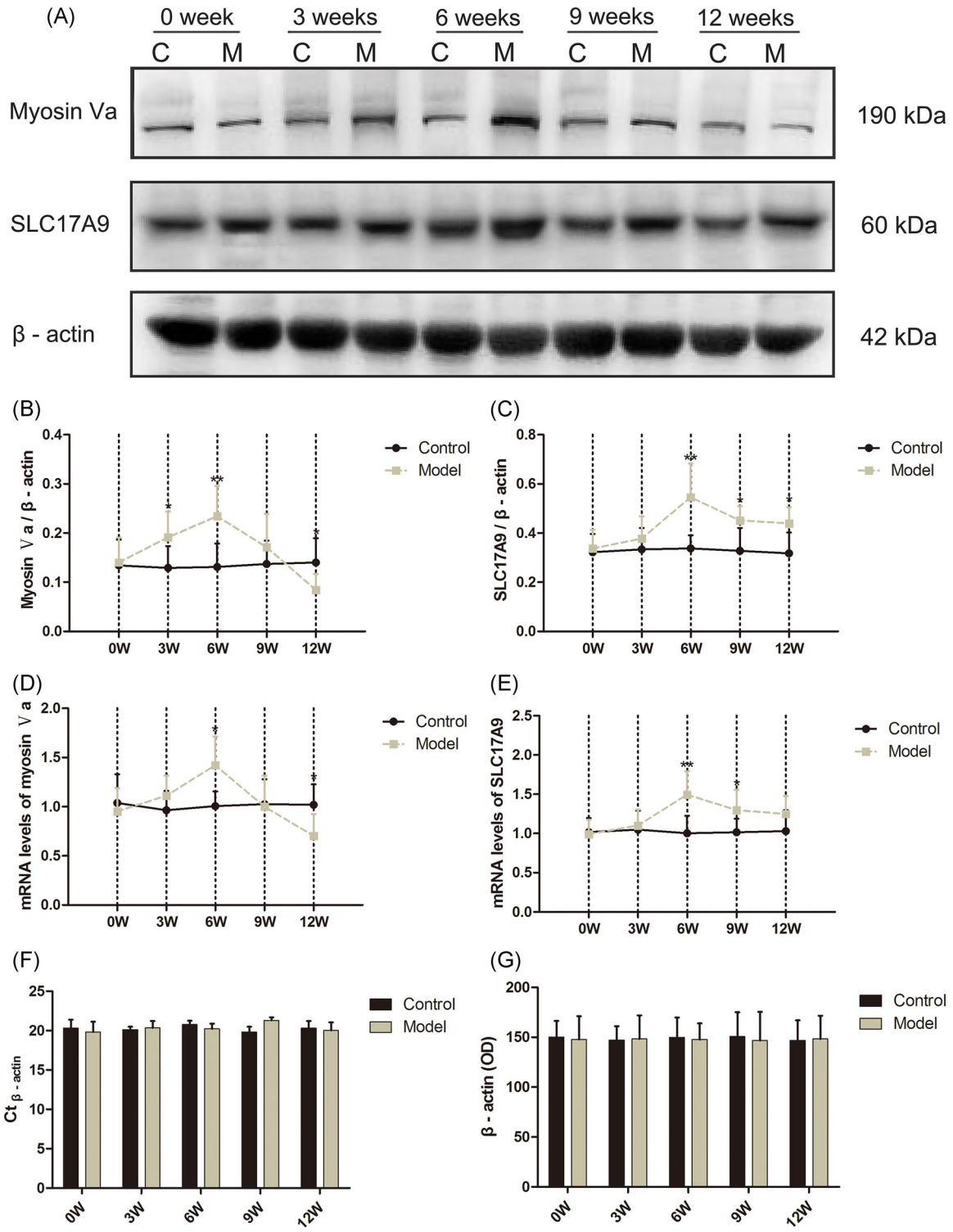

FIGURE 5 (A) Representative immunoblots of the protein expression levels of myosin Va, SLC17A9, and β-actin (n = 8). Quantification of protein expression levels of (B) myosin Va and (C) SLC17A9 by normalizing with β-actin, (G) optical density of protein for β-actin. Relative bladder mRNA expression levels for (D) myosin Va and (E) SLC17A9 in the age-matched control and DM mice from 0 to 12 weeks after the induction (n = 8), (F) Ct values of β-actin. Data represent the means ± SD (model vs control group, $^{*}P < 0.05$ or $^{**}P < 0.01$). DM, diabetes mellitus; mRNA, messenger RNA; SD, standard deviation

physical adaptation to an increased urine production and/or likely to induce an increased oxidative stress over time.

Contractility studies directly reflect the detrusor function and the contractility to respond to exogenous stimuli. In the current study, the amplitude of spontaneous activity significantly increased in an early state (at 3–6 weeks) but sharply decreased in the later state (at 12 weeks) in DM mice, in accordance with the results of previous reports.[10] In addition, similar to spontaneous activity, DMS strips contractile responses to α, β-methylene ATP, KCl, EFS, and carbachol stimulation are consistent with the "temporal hypothesis" in DM mice. And the results of contractility test are in line with the alternations in cystometric parameters at all points, thereby further supporting the fact that the "temporal hypothesis" applies to STZ-induced DM mice, and the transition from an overactive bladder to an atonic bladder is a gradual process that occurs approximately at 9 to 12 weeks after the DM induction. These findings are sufficiently intriguing and provide information for further investigation of the underlying molecular mechanisms of the compensation/decompensation in future experiments using DM models.

Bladder contraction is mainly mediated by purinergic and cholinergic pathways.[14] In healthy bladders, the contribution of ATP, which is the purinergic transmitter that activates P2X1 receptors causing contraction, is limited; However, the purinergic component accounts were radically changed in DM.[15] This insight paves the way to the exploration of the underlying molecular mechanism of purinergic pathway alternations in the DBD model. In addition, consistent with the previous studies' findings,[9,11] the EFS-induced DSM strip contractions that reflect the release amount of ATP and ACh from parasympathetic fibers markedly changed with time in DM mice. Furthermore, the contractile responses of DSM strips to α, β-methylene ATP were significantly changed in DM mice and rats, but no changes were found in mRNA expression levels for such receptors compared with those in the controls.[15] Hence, the alterations of bladder contractile function may be closely related to the change in the release amount of ATP and/or P2X1 receptors sensitivity in the bladder of DM mice. The release process of ATP, an important extracellular purinergic neurotransmitter, is mainly divided into two phases, namely, storage in secretory vesicles and exocytosis.[16] The phase of ATP storage in secretory vesicles is mediated by the VNUT, which is the product of the SLC17A9.[17] Next is the exocytosis phase in which ATP-filled vesicles are translocated to the varicosity membrane and carried by myosin motors (myosin Va is crucial) along the F-actin tracts; then, ATP is released at the varicosity membrane after undergoing Ca^2-dependent exocytosis.[18]

Myosin motors belong to a large superfamily of motor proteins,[23] which have unique molecular structures to transport distinctive cargoes, thereby ensuring that they meet the requirements for a multifarious physiological activity. Myosin Va is one of the most attractive motors distributed extensively in presynaptic and postsynaptic neurons. Therefore, we decided to evaluate the mRNA and protein expression levels for myosin Va and SLC17A9 in the bladder of DM mice. We found higher mRNA and protein expression levels of myosin Va and SLC17A9 at 6 weeks in DM mice, thereby suggesting that their upregulation may contribute to the increase in the ATP release. Such release is likely to induce an overactive bladder in DM at a compensatory state. Moreover, at 12 weeks, we detected sharply downregulated mRNA and protein expression levels of myosin Va in DM mice, which is possibly led to the transform, thereby conforming to the previous study.[24] Therefore, exploring drugs that can regulate the expression of myosin Va and SLC17A9 in the bladder may be an effective way to treat DBD clinically.

5 | CONCLUSION

In summary, the "temporal hypothesis" is consistent with the development process of DBD in STZ-induced DM mice, and the transition from a compensatory state to a decompensated state is approximately at 9 to 12 weeks after DM induction. Furthermore, the alternations of myosin Va and SLC17A9 expression levels with time contribute to the development of DBD in STZ-induced mice. This contribution is ideal for further investigation.

ACKNOWLEDGMENTS

The authors thank the School of Basic Medical Sciences, Guangzhou University of Chinese Medicine, for technical support. All experimental procedures were performed according to the ethical principle guidelines approved by the National Research Council. Male C57BL/6J mice were purchased from Beijing Vital River Laboratory Animal Technology Co., Ltd, China. Male C57BL/6J mice (18–22 g) were housed in the Experimental Animal Center of Guangzhou University of Chinese Medicine (No. S2017051, Guangzhou, China).

REAGENTS AND MATERIALS

STZ (TOKU-E Co., Ltd., Tokyo, Japan); α, β-methylene ATP (Tocris Bio-Techne Ltd., Minneapolis, MN);

Carbachol (Shandong Bausch & Lomb Freda Phar. Co., Ltd., Shanghai, China); FastKing One-step RT-PCR Kit and Talent qPCR PreMix (SYBR Green) (TIANGEN Biotech Co., Ltd., Beijing, China); TRIzol reagent (Thermo Fisher Scientific, MA); RIPA lysis buffer and protease inhibitor cocktail (100×) (CoWin Biosciences, Shanghai, China). BCA protein assay kit (Beyotime Biotechnology Co., Ltd., Shanghai, China). Chemiluminescent reagent (Millipore Co., Ltd., Germany). Lastly, all other reagents used were of analytical grade.

SPSS 19.0 (International Business Machines Corporation, NY); GraphPad Prism 5 (GraphPad Software, CA); ImageJ (National Institutes of Health, MA); Bio-Rad. Glob (Bio-Rad Laboratories, Inc.); Image Pro 6.0 (Media Cybernetics Co., Ltd., MA).

Accu-Chek Active Blood Glucose Meter (Roche Diagnostics, Basel, Switzerland); Microinjection pump (Smiths medical WZ-50C6, Zhejiang, China); Urodynamics meter (Laborite Delphis 94-R01-BT, Canada); Tissue grinders (Shanghai Jingxin, Shanghai, China); Electrochemiluminescence system (Tanon Science & Technology, Tanon-5200, Shanghai, China); Ultraviolet-spectrophotometer (Thermo Fisher Scientific, MA); GStorm Gradient PCR (Thermo Fisher Scientific); Real-time fluorescence quantitative PCR instrument (Thermo Fisher Scientific); Tissue dehydrator, Tissue embedding machine, paraffin slicing machine and Automatic tissue dyeing machine (Thermo Fisher Scientific).

FUNDING INFORMATION

This study was supported by the National Natural Science Foundation of China (grant no. 81673676) and Dongguan Science and Technology Bureau (grant no. 2019622101002).

ORCID

Hong-ying Cao http://orcid.org/0000-0001-6207-0168

REFERENCES

1. Karoli R, Bhat S, Fatima J, Priya S. A study of bladder dysfunction in women with type 2 diabetes mellitus. *Indian J Endocrinol Metab*. 2014;18(4):552.
2. Dong X, Song Q, Zhu J, et al. Interaction of Caveolin-3 and HCN is involved in the pathogenesis of diabetic cystopathy. *Sci Rep*. 2016;6:24844.
3. Frimodt-Möller CAI. Diabetic cystopathy.I: A clinical study of the frequency of bladder dysfunction in diabetics. *Dan Med Bull*. 1976;23(6):267-278.
4. Abrams P, Cardozo L, Fall M, et al. *The standardisation of terminology of lower urinary tract function*. Report from the standardisation sub-committee of the international continence society. Environmental Research Institute of Michigan; 2003.
5. Wein AJ. Classification of neurogenic voiding dysfunction. *J Urol*. 1981;125(5):605-609.
6. CAI Frimodt-Möller. Diabetic cystopathy: epidemiology and related disorders. *Ann Intern Med*. 1980;92(2 Pt 2):318-321.
7. Hunter KF, Moore KN. Diabetes-associated bladder dysfunction in the older adult (CE). *Geriatr Nurs (Minneap)*. 2003;24(3):138-145.
8. Leiria LOS, Monica FZ, Carvalho FD, et al. Functional, morphological and molecular characterization of bladder dysfunction in streptozotocin-induced diabetic mice: evidence of a role for L-type voltage-operated Ca2+channels. *Br J Pharmacol*. 2011;163(6):1276-1288.
9. Daneshgari F, Huang X, Bena G, Saffore J, Powell L, C. Temporal differences in bladder dysfunction caused by diabetes, diuresis, and treated diabetes in mice. *Am J Physiol: Regul, Integr Comp Physiol*. 2006;290(6):1728-1735.
10. Wang Z, Cheng Z, Cristofaro V, et al. Inhibition of TNF-α improves the bladder dysfunction that is associated with type 2 diabetes. *Diabetes*. 2012;61(8):2134-2145.
11. Daneshgari F, Liu G, Imrey PB. Time dependent changes in diabetic cystopathy in rats include compensated and decompensated bladder function. *J Urol*. 2006;176(1):380-386.
12. Daneshgari F, Liu G, Birder L, Hanna-Mitchell AT, Chacko S. Diabetic bladder dysfunction: current translational knowledge. *J Urol*. 2009;182(6):S18-S26.
13. Rue-Tsuan L, Min-Shen C, Wei-Chia L, et al. Prevalence of overactive bladder and associated risk factors in 1359 patients with type 2 diabetes. *J Urol*. 2011;78(5):1040-1045.
14. Zhengyong Y, Ziwei T, Changxiao H, Wei T. Diabetic cystopathy: A review. *J Diabetes*. 2015;7(4):442-447.
15. Lo L, Fz M, Fd C, et al. Functional, morphological and molecular characterization of bladder dysfunction in streptozotocin-induced diabetic mice: evidence of a role for L-type voltage-operated Ca2+channels. *Br J Pharmacol*. 2011;163(6):1276-1288.
16. Yolanda GM, Diego B, Rosa GV, et al. P2X7 receptors trigger ATP exocytosis and modify secretory vesicle dynamics in neuroblastoma cells. *J Biol Chem*. 2011;286(13):11370-11381.
17. Keisuke S, Noriko E, Narinobu J, et al. Identification of a vesicular nucleotide transporter. *Proc Natl Acad Sci USA*. 2008;105(15):5683-5686.
18. Chaudhury A, He XD, Goyal RK. Role of myosin Va in purinergic vesicular neurotransmission in the gut. *American Journal of Physiology Gastrointestinal & Liver Physiology*. 2012;302(6):G598-G607.
19. Lai H, Yan QT, Cao H, et al. Effect of SQW on the bladder function of mice lacking TRPV1. *Bmc Complementary & Alternative Medicine*. 2016;16(1):465.
20. Wein AJ. Urinary incontinence: classification and therapeutic guidelines. *Semin Urol*. 1989;7(2):59-64.
21. Arioglu Inan E, Ellenbroek JH, Michel MC. A systematic review of urinary bladder hypertrophy in experimental

diabetes: Part I. Streptozotocin-induced rat models. *Neurourol Urodyn*. 2018;37(4):1212-1219.
22. Ellenbroek JH, Arioglu Inan E, Michel MC. A systematic review of urinary bladder hypertrophy in experimental diabetes: Part 2. Comparison of animal models and functional consequences. *Neurourology and Urodynamics*. 2018;37(8): 2346-2360.
23. Foth BJ, Goedecke MC, Soldati D. New insights into myosin evolution and classification. *Proc Natl Acad Sci USA*. 2006;103(10):3681-3686.
24. Chaudhury A, De Miranda-Neto MH, Pereira RV, Zanoni JN. Myosin Va but not nNOSalpha is significantly reduced in jejunal musculomotor nerve terminals in diabetes mellitus. *Front Med*. 2014;1:17.

SUPPORTING INFORMATION

Additional supporting information may be found online in the Supporting Information section at the end of the article.

How to cite this article: Yang Xf, Wang J, Rui-Wang, et al. Time-dependent functional, morphological, and molecular changes in diabetic bladder dysfunction in streptozotocin-induced diabetic mice. *Neurourology and Urodynamics*. 2019; 38:1266-1277. https://doi.org/10.1002/nau.24008